

# Discovery of Heteroatom-“Embedded” $\text{Te} \subset \{\text{W}_{18}\text{O}_{54}\}$ Nanofunctional Polyoxometalates by Use of Cryospray Mass Spectrometry\*\*

Jun Yan, De-Liang Long,\* Elizabeth F. Wilson, and Leroy Cronin\*

Polyoxometalates (POMs) are fascinating metal oxide cluster compounds with applications in many fields, from medicine to nanotechnology.<sup>[1–8]</sup> In POM chemistry, countless new structural types have been synthesized and characterized,<sup>[4–10]</sup> but there is a need to develop new synthetic routes to allow the development of tunable and functional cluster systems.<sup>[11,12]</sup> We have been targeting cluster cage template systems whereby new guest species, such as  $\text{WO}_6^{6-}$  and  $\text{IO}_6^{5-}$ , are inserted into a  $\{\text{M}_{18}\text{O}_{54}\}$  cage.<sup>[13]</sup> The  $\{\text{M}_{18}\text{O}_{54}\}$  cluster cage ( $\text{M} = \text{Mo}$  or  $\text{W}$ ) has many versatile features, such as electronic configurability or use as a synthetic platform, which should allow the design of novel functional nano-objects. Although the crystallization-based approach to cluster discovery has transformed the field, the direct unambiguous discovery of new clusters in a given reaction system is difficult. This difficulty arises because of the need to correlate the synthetic parameters with the cluster structure, requiring cycles of synthesis, crystallization, and structural characterization.

Herein we present a new approach to the discovery of cage-template nanoclusters, which utilizes cryospray mass spectrometry (CSI-MS)<sup>[14]</sup> to directly probe the reaction solution, thereby allowing the process to be accomplished much more quickly and facilitating the discovery of new guests inside nanocluster cage architectures (Scheme 1).

We targeted the encapsulation of  $\{\text{TeO}_6\}^{6-}$  units within  $\{\text{W}_{18}\text{O}_{54}\}$  cluster shells to give the tellurate-based Dawson-like anion because, although this process should be straightforward according to our previous work,<sup>[13]</sup> we found that it was

not possible to synthesize these new clusters using the conventional approach. However, by probing the reaction mixture with CSI-MS, we were able to screen different cation systems. Of the cations screened, dimethylammonium ( $\text{DMAH}^+$ ) and tetrabutylammonium ( $\text{TBA}^+$ ) were successful, yielding  $[\text{H}_3\text{W}_{18}\text{O}_{56}(\text{TeO}_6)]^{7-}$  (**1a**; Figure 1) as  $\text{Na}(\text{DMAH})_6[\text{H}_3\text{W}_{18}\text{O}_{56}(\text{Te}^{\text{VI}}\text{O}_6)] \cdot 14\text{H}_2\text{O}$  **1** and  $(\text{TBA})_7[\text{H}_3\text{W}_{18}\text{O}_{56}(\text{Te}^{\text{VI}}\text{O}_6)] \cdot 4\text{CH}_3\text{CN}$  **1'**,<sup>[15]</sup> respectively. Furthermore, the activation of the cluster cage by the Te heteroanion is demonstrated by the reduction of the tellurate  $\{\text{Te}^{\text{VI}}\text{O}_6\}$  within **1a** to tellurite  $\{\text{Te}^{\text{IV}}\text{O}_3\}$ , thereby transforming **1a**, to

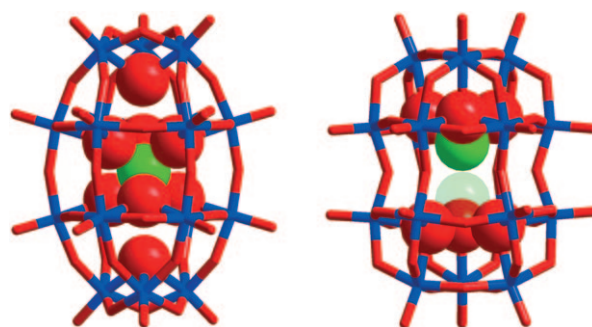
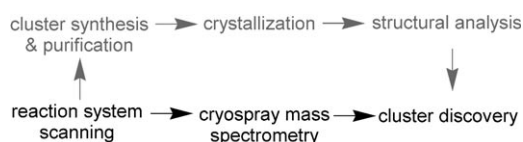


**Figure 1.** Structures of **1a**  $[\text{H}_3\text{Te}^{\text{VI}}\text{W}_{18}\text{O}_{62}]^{7-}$  (left) and **2a**  $[\text{H}_3\text{Te}^{\text{IV}}\text{W}_{18}\text{O}_{60}]^{5-}$  (right). The  $\{\text{W}_{18}\}$  cages are shown as stick models and the central  $\{\text{TeO}_x\}$  group is shown in space-filling mode, as are the two oxo ligands which are lost from the oxidized structure (**1a**) upon reduction. O red; Te green; W blue. H atoms are omitted for clarity.



**Scheme 1.** The three steps for conventional cluster discovery compared to the one-step approach using cryospray mass spectrometry.

$[\text{H}_3\text{W}_{18}\text{O}_{57}(\text{Te}^{\text{IV}}\text{O}_3)]^{5-}$ , (**2a**; Figure 1) without decomposition of the cluster cage. Cluster **2a** has also been isolated in the solid state as  $(\text{TBA})_5[\text{H}_3\text{W}_{18}\text{O}_{57}(\text{Te}^{\text{IV}}\text{O}_3)]$  **2**, in which the pyramidal tellurite anion  $[\text{Te}^{\text{IV}}\text{O}_3]^{2-}$  acts as a template supporting the  $\{\text{W}_{18}\text{O}_{54}\}$  cage. This redox reaction, which transforms **1a** into **2a**, can be monitored in situ by use of CSI-MS. Finally, the inclusion of the Te-based heteroanion activates the surface of the  $\{\text{W}_{18}\text{O}_{54}\}$  cluster cage, facilitating the assembly of the cluster to nanoscale structures without the introduction of other transition metal electrophiles, with two  $\{\text{W}_{18}\text{Te}^{\text{VI}}\}$  units linked together by two  $\{\text{W}_{11}\}$  units to give  $[\text{H}_{10}\text{Te}^{\text{VI}}_2\text{W}_{58}\text{O}_{198}]^{26-}$  **3a**, which was isolated as  $\text{Na}_8(\text{DMAH})_{18}[\text{H}_{10}\text{Te}^{\text{VI}}_2\text{W}_{58}\text{O}_{198}] \cdot 35\text{H}_2\text{O}$  **3** in the solid state. Compounds **1–3** were fully characterized by use of elemental analysis and single-crystal structure determination, and compounds **1** and **2** were detected by use of CSI-MS.

The participation of tellurate and tellurite as heteroanions in POM chemistry is reasonably well known: tellurate is employed in the formation of the Anderson-type cluster  $\{\text{Te}^{\text{VI}}\text{M}_6\}$  ( $\text{M} = \text{Mo}$  or  $\text{W}$ )<sup>[16,17]</sup> and tellurite in the  $\{\text{Te}^{\text{IV}}\text{W}_9\}$

[\*] J. Yan, Dr. D.-L. Long, E. F. Wilson, Prof. Dr. L. Cronin WestCHEM, Department of Chemistry, The University of Glasgow University Avenue, Glasgow G12 8QQ, Scotland (UK) Fax: (+44) 141-330-4888 E-mail: longd@chem.gla.ac.uk l.cronin@chem.gla.ac.uk Homepage: <http://www.chem.gla.ac.uk/staff/lee> <http://www.chem.gla.ac.uk/~longd>

[\*\*] We thank the EPSRC, the Chinese Scholarship Council, WestCHEM and the University of Glasgow for supporting this work.

Supporting information for this article is available on the WWW under <http://dx.doi.org/10.1002/anie.200806343>.

building blocks that form a variety of metal complexes, such as  $[\text{Te}_2\text{W}_{18}\text{Cu}_3\text{O}_{66}(\text{H}_2\text{O})_3]^{10-}$ ,  $[\text{Fe}_4(\text{H}_2\text{O})_{10}(\text{TeW}_9\text{O}_{33})_2]^{4-}$ , and  $[\text{M}_3(\text{H}_2\text{O})_8(\text{WO}_2)(\text{TeW}_9\text{O}_{33})_2]^{n-}$  ( $\text{M} = \text{V}^{\text{IV}}$ ,  $\text{Co}^{\text{II}}$ ,  $\text{Zn}^{\text{II}}$ , or  $\text{Ni}^{\text{II}}$ ).<sup>[18,19]</sup> However, to our knowledge, compounds **1**, **1'**, **2**, and **3** represent the first examples of tellurate and tellurite embedded within the Dawson-type  $\{\text{W}_{18}\text{O}_{54}\}$  matrix, and thus offer the potential to develop new chemical and physical properties derived from the well-known conventional Dawson cluster structure type.

Cluster **1** was discovered in a reaction system containing  $\text{Na}_2\text{WO}_4$  and  $\text{Te}(\text{OH})_6$  at pH 0.8 in the presence of DMA. The presence of DMA is crucial since its absence leads exclusively to the formation of the Anderson-type cluster  $[\text{TeW}_6\text{O}_{24}]^{6-}$ , which reiterates the pivotal effect of employing organic cations for the assembly of new POMs.<sup>[11,12]</sup> X-ray crystallographic structure analysis of **1** revealed a Dawson-type  $D_{3d}$ -symmetric  $\{\text{W}_{18}\text{O}_{54}\}$  cluster shell enclosing a  $D_{3d}$ -symmetric  $\{\text{TeO}_6\}$  unit with an average Te–O distance of 1.98(2) Å and an average TeO–W distance of 2.34(2) Å. The two additional interior oxygen positions each bridge one of the capping  $\{\text{W}_3\}$  groups of the clusters, with an average W–O distance of 2.24(2) Å. The cluster represents a  $\gamma^*$ -isomer in the family of  $\{\text{W}_{18}\}$  Dawson-type structures (Figure 1).<sup>[13]</sup>

The structure of the cluster  $\gamma^*[\text{H}_3\text{W}_{18}\text{O}_{56}(\text{Te}^{\text{VI}}\text{O}_6)]^{7-}$  **1a** is similar to that of the  $\beta^*[\text{H}_3\text{W}_{18}\text{O}_{56}(\text{IO}_6)]^{6-}$ , with Te or I located at the cluster centers (Figure 1). For conventional Dawson heteropolyanions, each of the two tetrahedral cavities are normally occupied by a heteroatom, but in the  $\{\text{W}_{18}\text{X}\}$  systems, wherein there is only one central heteroatom, structural and bond valence sum analyses suggest that these tetrahedral positions are occupied instead by protons.<sup>[15]</sup> The Te-containing structure (Figure 1) adopts a  $\gamma^*$  conformation, whereas the I-containing structure has a  $\beta^*$  conformation. One major difference between the two isomers is the orientation of the three capping W metal centers, and in the  $\beta^*$  isomer the  $\{\text{W}_{18}\text{O}_{54}\}$  cluster shell is  $D_{3h}$ -symmetric.<sup>[13]</sup> In this work we were only able to discover the correct synthetic route to the  $\text{TeC}\{\text{W}_{18}\text{O}_{54}\}$  compound type by use of CSI-MS, which then allowed isolation and crystallographic analysis of the pure compound. This analysis was important also because the heteroatom was located on a crystallographic threefold axis, and the CSI-MS data allowed us to rule out the possibility that the central template could be  $\{\text{WO}_6\}$ , which would have implied the cluster could be formulated as  $[\text{H}_4\text{W}_{19}\text{O}_{62}]$ .<sup>[20–22]</sup> CSI mass spectra of compound **1'** showed four characteristic peaks at  $m/z$  2822.5 ( $[(\text{TBA})_5\text{H}_3\text{Te}^{\text{VI}}\text{W}_{18}\text{O}_{62}]^{2-}$ ), 2701.4 ( $[(\text{TBA})_4\text{H}_4\text{Te}^{\text{VI}}\text{W}_{18}\text{O}_{62}]^{2-}$ ), 3065.4 ( $[(\text{TBA})_7\text{H}_5\text{Te}^{\text{VI}}\text{W}_{18}\text{O}_{62}]^{2+}$ ), and 3186.0 ( $[(\text{TBA})_8\text{H}_4\text{Te}^{\text{VI}}\text{W}_{18}\text{O}_{62}]^{2+}$ ). In contrast, the mass spectrum of the TBA salt of the  $[\text{H}_4\text{W}_{19}\text{O}_{62}]^{6-}$  anion showed quite different peaks at  $m/z$  2729.9 ( $[(\text{TBA})_4\text{H}_4\text{W}_{19}\text{O}_{62}]^{2-}$ ) and 2850.6 ( $[(\text{TBA})_5\text{H}_3\text{W}_{19}\text{O}_{62}]^{2-}$ ).

We examined the reduction of cluster **1a**, to test whether we could access a  $\text{Te}^{\text{IV}}$ -based species.<sup>[25]</sup> On addition of solid  $\text{Na}_2\text{S}_2\text{O}_4$  to the acidified solution of compound **1**, the solution initially turned blue, owing to the reduction of the  $\{\text{W}_{18}\}$ -based cluster shell, and then became pale yellow within seconds. We postulated that the central Te was reduced in this process from  $\text{Te}^{\text{VI}}$  to  $\text{Te}^{\text{IV}}$ . This reduction was confirmed by

isolation of **2a**, by precipitation with  $\text{TBA}^+$ , and this material was subsequently crystallized from acetonitrile to yield **2**. Single-crystal X-ray diffraction analysis of **2** revealed that the  $\text{Te}^{\text{IV}}$  center had shifted by 1.10 Å towards one end of the cluster to form a pyramidal tellurite ion. Upon formal two-electron reduction, the central octahedral  $\{\text{Te}^{\text{VI}}\text{O}_6\}^{6-}$  unit was transformed into a pyramidal  $\{\text{Te}^{\text{IV}}\text{O}_3\}^{2-}$  unit with the breaking of three W–O bonds. The two interior “capping” oxo ligands were also lost in this reduction process. The resulting cluster that contained the  $\text{Te}^{\text{IV}}$  center had pseudo  $D_{3d}$  symmetry, with the sole Te atom disordered over two possible positions, approximately 2.20 Å apart, an average Te–O distance of 1.90 Å, and an average TeO–W distance of 2.31 Å (Figure 1). Cluster **2a** had a similar structure to its Sb analogue  $[\text{H}_2\text{W}_{18}\text{O}_{57}(\text{Sb}^{\text{III}}\text{O}_3)]^{7-}$ .<sup>[20]</sup>

The composition of cluster **2a**, was confirmed by use of high-resolution CSI-MS experiments, which gave rise to peaks corresponding the cluster  $\{\text{W}_{18}\text{Te}^{\text{IV}}\}$ ;  $m/z$  (expected values and anion composition in parentheses): 2573.9 (2574.3;  $[\text{Na}(\text{TBA})_3\text{H}_2\text{W}_{18}\text{Te}^{\text{IV}}\text{O}_{60}]^{2-}$ ), 2563.0 (2563.3;  $[(\text{TBA})_3\text{H}_3\text{W}_{18}\text{Te}^{\text{IV}}\text{O}_{60}]^{2-}$ ), 2433.8 (2433.7;  $[(\text{TBA})_2\text{H}_2\text{W}_{18}\text{Te}^{\text{IV}}\text{O}_{59}]^{2-}$ ), 2684.5 (2684.4;  $[(\text{TBA})_4\text{H}_2\text{W}_{18}\text{Te}^{\text{IV}}\text{O}_{60}]^{2-}$ ), 1708.6 (1708.5;  $[(\text{TBA})_3\text{H}_2\text{W}_{18}\text{Te}^{\text{IV}}\text{O}_{60}]^{3-}$ ).

Further investigation of the tungstate–tellurate reaction-parameter space revealed that, by adjusting the solution to approximately pH 2, it was possible to form a nanosized crown-like tetrameric heteropolytungstate cluster **3a**, approximately  $1.9 \times 2.9$  nm in size, which was isolated as a crystalline product. Single-crystal X-ray diffraction analysis of **3** shows the cluster is composed of two  $\{\text{TeW}_{18}\text{O}_{62}\}$  and two  $\{\text{W}_{11}\text{O}_{38}\}$  subunits that are linked together by corner-sharing  $\text{WO}_6$  octahedra (Figure 2).

The structure of the  $\{\text{W}_{11}\text{O}_{38}\}$  unit in **3a** is similar to the known cluster  $[\text{H}_4\text{W}_{11}\text{O}_{38}]^{6-}$ <sup>[23]</sup> and the  $\{\text{W}_{11}\}$  building blocks found in the isopolyoxotungstate clusters  $[\text{H}_4\text{W}_{22}\text{O}_{74}]^{12-}$  and  $[\text{H}_{10}\text{W}_{34}\text{O}_{116}]^{18-}$ .<sup>[24]</sup> To allow the linkage from the  $\{\text{W}_{11}\}$  unit, two adjacent belt W centers on each of the  $\{\text{TeW}_{18}\}$  clusters are shifted towards the outside of the cluster from normal positions found in a conventional “closed” Dawson-type  $\{\text{W}_{18}\text{O}_{54}\}$  cage, whereby the belt W–O–W bridge is missing and the Dawson-type clusters are pried apart (i.e. the W–O–W bond is broken) and distorted to give a window (Figure 2). The two metal centers across the window are 5.1 Å apart, which is much longer than the normal belt W–W distance of 3.4 Å in the normal  $\text{W}_{18}$  cage. The heteroanion  $\text{TeO}_6^{6-}$  remains at the center of the distorted  $\{\text{W}_{18}\}$  cage in a non-ideal octahedral geometry with Te–O distances in the range 1.90–2.00 Å. Compound **3a** represents a rare, if not the first ever nonlacunary polyoxotungstate to be linked without the need for additional electrophilic linkers, which has great potential for the future design and assembly of large POM nanostructures.

By utilizing high resolution CSI-MS for the real-time examination of the reactivity of the clusters, we were even able to monitor the transformation process from **1a** to **2a**, which involves the structural and electronic rearrangement of the Te-based template within the  $\{\text{W}_{18}\}$ -based cage, from  $[\text{Te}^{\text{VI}}\text{O}_6]^{6-}$  in **1a** to  $[\text{Te}^{\text{IV}}\text{O}_3]^{2-}$  in **2a**. In this experiment, an acetonitrile solution of compound **1'** was infused into the mass

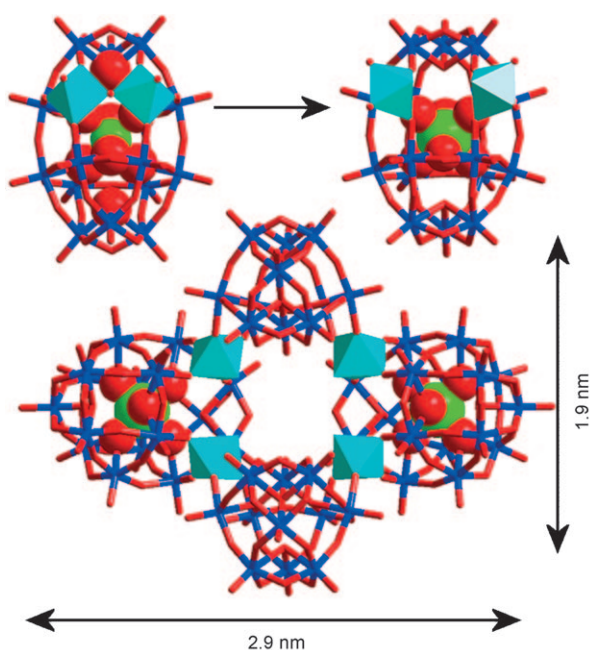


**Figure 2.** Top: The  $\{W_{18}Te\}$  precursor in **1** (left) and that in **3a** (right). In both representations, the W octahedra which fold out to form links to the  $\{W_{11}\}$  units are shown as light blue polyhedra. Bottom: Structure of **3a**  $[H_{10}Te^{VI}_2W_{58}O_{198}]^{26-}$ . The structures are shown as stick models with the linking  $\{WO_6\}$  units as light blue polyhedra, and the embedded  $\{TeO_6\}$  groups as space-filling models. O red; Te green; W blue. H atoms are omitted for clarity.

spectrometer along with stream of highly diluted  $Na_2S_2O_4$  solution in acetonitrile/water (95:5 v/v) with concurrent CSI-MS measurements. We were able to observe the reduction by changes in the mass spectrum from that of **1** to that of **2** (Figure 3), with no additional fragmentation associated with decomposed cluster cages, such as  $\{W_9\}$ , or other species. These results point to an intramolecular redox transformation that does not require the decomposition and reassembly of the cluster cage. Such decomposition/reassembly is unlikely to happen in acetonitrile solution at such a high rate and no fragments that relate to cluster decomposition are detected.<sup>[26]</sup> However, the loss of the two interior oxo ligands accompany-

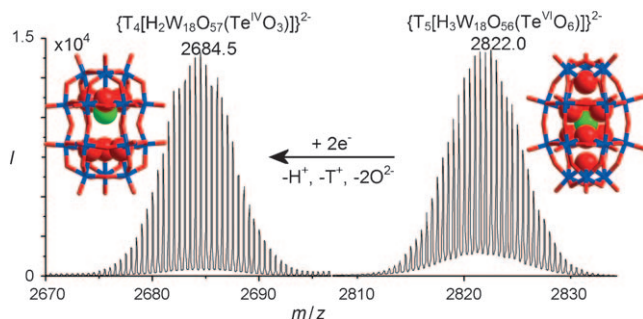


**Figure 3.** Characteristic peaks measured before (right) and after (left) the reduction of  $Te^{VI}$  to  $Te^{IV}$ , monitored by in situ mass spectrometry. ( $T \equiv TBA^+$ ). Inset structures of the oxidized and reduced species are shown.

ing the fast reduction process is unprecedented (see the Supporting Information).

The CSI-MS studies also showed that the cluster  $\{W_{18}Te^{VI}\}$  is present as both three- and fourfold protonated forms in acetonitrile solution. Furthermore, this information, when combined with the crystallographic and elemental analysis data, allows us to unambiguously assign the protonation state of the clusters in the solid state; for **1a** this is  $[H_3W_{18}O_{56}(Te^{VI}O_6)]^{7-}$ . This state is not unusual and a similar pattern is seen for **2a**, which is both two- and threefold protonated in solution, but  $[H_3W_{18}O_{57}(Te^{IV}O_3)]^{5-}$  is the major solid-state form, as confirmed by elemental and crystallographic analyses. Notably, in the mass spectrum of **1'**, some shoulder peaks, for example, that at  $m/z$  2692.9 (corresponding to  $\{(TBA)_4[H_2Te^{VI}W_{18}O_{61}]^{2-}\}$ ) are observed beside the major peaks, for example that at  $m/z$  2701.4 (corresponding to  $\{(TBA)_4[H_4Te^{VI}W_{18}O_{62}]^{2-}\}$ ). The  $m/z$  difference of nine clearly indicates the loss of one  $H_2O$  molecule from the cluster cage. We have detected such behavior before in ESI-MS studies for protonated POM clusters, such as  $[H_4W_{19}O_{62}]^{6-}$  and  $[H_3W_{18}O_{56}(IO_6)]^{6-}$ .<sup>[13,14]</sup>

In summary, we have discovered a new type of tungstotellurate compound by use of solution-state CSI-MS, which allowed us to isolate  $\gamma^*-[H_3W_{18}O_{56}(Te^{VI}O_6)]^{7-}$ , with a tellurate anion embedded within the  $\{W_{18}O_{54}\}$  Dawson-type shell. Selective reduction of the heteroatom yielded  $[H_3W_{18}Te^{IV}O_{60}]^{5-}$ , which resulted in both electronic and structural reorganizations of the Te-based ion within the cluster shell. Control of the solution pH allowed us to assemble a nanosized high nuclearity POM heteropolytungstate  $[H_{10}Te^{VI}_2W_{58}O_{198}]^{26-}$ , based on  $\{Te^{VI}W_{18}\}$  cluster cages, without the need to incorporate additional electrophilic linkers. The incorporation of Te gave access to clusters with significantly different chemical and physical properties compared to conventional heteropolyoxometalate clusters, as well as allowing us to monitor, by use of mass spectrometry, a redox reaction involving the transformation of the templating heteroanion from  $[Te^{VI}O_6]^{6-}$  to  $[Te^{IV}O_3]^{2-}$ . The polarization that results from the movement of the Te atom from the center of cluster **1a** closer to one end of cluster **2a** gives the cluster an asymmetric charge distribution that is manifested directly in the crystallization of **2**, in which **2a** is arranged in a polar chiral space group,  $I_4$ , which demonstrates potential for use as a polar material. In the future we are looking to develop the cryospray cluster-discovery process further, as well as exploiting the novel properties arising from the incorporation of heteroanions within polyoxometalate nanocages, for the design of nanoscale devices, materials, and new types of redox reagents.

### Experimental Section

**1:**  $Na_2WO_4 \cdot 2H_2O$  (20.0 g, 60.6 mmol) and dimethylamine hydrochloride (8.1 g, 100 mmol) were dissolved in water (50 mL) and  $Te(OH)_6$  (1.0 g, 4.35 mmol) was added and dissolved. The pH was adjusted to 0.8 by addition of aqueous 6 M HCl. The solution was heated at reflux for 2 h and then allowed to cool to room temperature, before the solvent was allowed to evaporate slowly. Compound **1** appeared as light yellow block crystals within one week (3.8 g, 0.76 mmol, 23.7% based on W). IR (KBr disk):  $\tilde{\nu} = 3449, 3143, 2791, 1622, 1464, 1402$ ,

1019, 949, 799  $\text{cm}^{-1}$ . Elemental analysis calcd (%) for  $\text{Na}_{12}\text{H}_{51}\text{N}_6\text{W}_{18}\text{TeO}_{62}$ : C 3.05, H 1.11, N 1.78, Na 0.49, Te 2.70, W 69.9; found C 3.27, H 1.26, N 1.88, Na 0.56, Te 2.66, W 70.9.

**1'**:  $(\text{DMAH})_6\text{Na}[\text{H}_3\text{W}_{18}\text{O}_{56}(\text{Te}^{\text{VI}}\text{O}_6)]$  (1.8 g, 0.36 mmol) was dissolved in water (20 mL). Tetrabutylammonium bromide (5.0 g, 20.6 mmol) dissolved in water (20 mL) was added with stirring. The resultant precipitate was centrifuged and washed with water, ethanol, and ether, and dried under reduced pressure. Recrystallization from acetonitrile afforded the pure product **1'** (1.0 g, 0.15 mmol, 49.8% based on W). IR (KBr disk):  $\tilde{\nu} = 3412, 2961, 2933, 2871, 1636, 1483, 1379, 1016, 947.8, 812 \text{ cm}^{-1}$ . Elemental analysis calcd (%) for  $\text{C}_{112}\text{H}_{255}\text{N}_7\text{W}_{18}\text{TeO}_{62}$ : C 21.95, H 4.19, N 1.60; found C 21.54, H 4.29, N 1.70.

**2**:  $(\text{DMAH})_6\text{Na}[\text{H}_3\text{W}_{18}\text{O}_{56}(\text{Te}^{\text{VI}}\text{O}_6)]$  (2.0 g, 0.40 mmol) was dissolved in 0.1 M aqueous HCl (50 mL), and  $\text{Na}_2\text{S}_2\text{O}_4$  (0.1 g, 0.58 mmol) was added with stirring. Tetrabutylammonium bromide (5.0 g, 20.6 mmol) dissolved in water (20 mL) was added. The resultant precipitate was centrifuged and washed with water, ethanol, and ether, and dried under vacuum. Dissolution of the solid in acetonitrile led to two crystal morphologies. Colorless star-shaped crystals were separated from the pale yellow needle-like crystals of  $(\text{TBA})_7[\text{H}_3\text{W}_{18}\text{O}_{56}(\text{Te}^{\text{VI}}\text{O}_6)]$ , and were then purified by a second recrystallization from acetonitrile to yield **2** as colorless block crystals (0.5 g, 0.088 mmol, 24.5%). IR (KBr disk):  $\tilde{\nu} = 3446, 2961, 2932, 2873, 1636, 1483, 1379, 1152, 977, 900, 807 \text{ cm}^{-1}$ . Elemental analysis calcd (%) for  $\text{C}_{80}\text{H}_{185}\text{N}_5\text{W}_{18}\text{TeO}_{60}$ : C 17.12, H 3.29, N 1.25%; found C 17.47, H 3.25, N 1.31%.

**3**:  $\text{Na}_2\text{WO}_4 \cdot 2\text{H}_2\text{O}$  (20.0 g, 60.6 mmol) and dimethylamine hydrochloride (8.1 g, 100 mmol) were dissolved in water (50 mL) and  $\text{Te}(\text{OH})_6$  (1.0 g, 4.35 mmol) was added and dissolved. The pH was adjusted to 2.0 by addition of 37% HCl and the solution was heated until it began to turn yellow. The solution was then allowed to cool to room temperature and the solvent was allowed to evaporate slowly. Pure compound **3** appeared within one week as colorless branch-like crystals (0.6 g, 0.038 mmol, 3.8% based on W). IR (KBr disk):  $\tilde{\nu} = 3424, 3132, 2776, 2427, 1609, 1462, 1411, 1248, 1018, 950, 799, 737 \text{ cm}^{-1}$ . Elemental analysis calcd (%) for  $\text{Na}_8\text{C}_36\text{H}_{154}\text{N}_{18}\text{W}_{58}\text{Te}_2\text{O}_{198}$ : C 2.86, H 1.03, N 1.67, Na 1.22, Te 1.69, W 70.6%; found C 3.02, H 1.50, N 1.87, Na 1.08, Te 1.56, W 70.9%.

Received: December 28, 2008

Revised: March 20, 2009

Published online: May 11, 2009

**Keywords:** cluster compounds · mass spectrometry · polyoxometalates · redox chemistry · tungsten

- [1] a) D. L. Long, E. Burkholder, L. Cronin, *Chem. Soc. Rev.* **2007**, 36, 105; b) Special Thematic Issue on Polyoxometalate (Ed.: C. L. Hill): *Chem. Rev.* **1998**, 98; c) M. T. Pope, A. Müller, *Polyoxometalate Chemistry: From Topology via Self-Assembly to Applications*, Kluwer, Dordrecht, **2001**; d) M. T. Pope, A. Müller, *Angew. Chem.* **1991**, 103, 56; *Angew. Chem. Int. Ed. Engl.* **1991**, 30, 34.
- [2] A. Dolbecq, C. Mellot-Draznieks, P. Mialane, J. Marrot, G. Férey, F. Sécheresse, *Eur. J. Inorg. Chem.* **2005**, 3009.
- [3] B. Hasenknopf, *Front. Biosci.* **2005**, 10, 275.
- [4] T. M. Anderson, W. A. Neiwert, M. L. Kirk, P. M. B. Piccoli, A. J. Schultz, T. F. Koetzle, D. G. Musaev, K. Morokuma, R. Cao, C. L. Hill, *Science* **2004**, 306, 2074.
- [5] L. Yan, X. López, J. J. Carbó, R. Sniatynsky, D. C. Duncan, J. M. Poblet, *J. Am. Chem. Soc.* **2008**, 130, 8223.
- [6] A. Müller, E. Beckmann, H. Bögge, M. Schmidtman, A. Dress, *Angew. Chem.* **2002**, 114, 1210; *Angew. Chem. Int. Ed.* **2002**, 41, 1162.

- [7] J. Lehmann, A. Gaita-Arino, E. Coronado, D. Loss, *Nat. Nanotechnol.* **2007**, 2, 312.
- [8] a) A. Sartorel, M. Carraro, G. Scorrano, R. D. Zorzi, S. Geremia, N. D. McDaniel, S. Bernhard, M. Bonchio, *J. Am. Chem. Soc.* **2008**, 130, 5006; b) Y. V. Geletii, B. Botar, P. Kögerler, D. A. Hillesheim, D. G. Musaev, C. L. Hill, *Angew. Chem.* **2008**, 120, 3960; *Angew. Chem. Int. Ed.* **2008**, 47, 3896.
- [9] a) U. Kortz, M. T. Pope, *Inorg. Chem.* **1994**, 33, 5643; b) A. Müller, E. Krickemeyer, J. Meyer, H. Bögge, F. Peters, W. Plass, E. Diemann, S. Dillinger, F. Nonnenbruch, M. Randerath, C. Menke, *Angew. Chem.* **1995**, 107, 2293; *Angew. Chem. Int. Ed. Engl.* **1995**, 34, 2122.
- [10] a) S. G. Mitchell, C. Ritchie, D. L. Long, L. Cronin, *Dalton Trans.* **2008**, 1415; b) Y. F. Song, N. McMillan, D. L. Long, J. Thiel, Y. L. Ding, H. S. Chen, N. Gadegaard, L. Cronin, *Chem. Eur. J.* **2008**, 14, 2349.
- [11] D. L. Long, P. Kögerler, L. J. Farrugia, L. Cronin, *Angew. Chem.* **2003**, 115, 4312; *Angew. Chem. Int. Ed.* **2003**, 42, 4180.
- [12] D. L. Long, P. Kögerler, L. Cronin, *Angew. Chem.* **2004**, 116, 1853; *Angew. Chem. Int. Ed.* **2004**, 43, 1817.
- [13] a) D. L. Long, P. Kögerler, A. D. C. Parenty, J. Fielden, L. Cronin, *Angew. Chem.* **2006**, 118, 4916; *Angew. Chem. Int. Ed.* **2006**, 45, 4798; b) D. L. Long, Y. F. Song, E. F. Wilson, P. Kögerler, S. X. Guo, A. M. Bond, J. S. J. Hargreaves, L. Cronin, *Angew. Chem.* **2008**, 120, 4456; *Angew. Chem. Int. Ed.* **2008**, 47, 4384.
- [14] H. N. Miras, E. F. Wilson, L. Cronin, *Chem. Commun.* **2009**, 1297.
- [15] Crystal data and structure refinement: **1**:  $\text{C}_{12}\text{H}_9\text{N}_6\text{NaO}_7\text{Te}_1\text{W}_{18}$ ;  $M_r = 4983.70$ ; crystal size  $0.23 \times 0.19 \times 0.11 \text{ mm}$ ;  $T = 150(2) \text{ K}$ ; trigonal; space group  $R\bar{3}m$ ;  $a = 20.7816(5)$ ,  $c = 17.0359(5) \text{ \AA}$ ;  $V = 6371.7(3) \text{ \AA}^3$ ;  $Z = 3$ ;  $\rho = 3.896 \text{ g cm}^{-3}$ ;  $\mu(\text{MoK}\alpha) = 24.712 \text{ mm}^{-1}$ ;  $F(000) = 6588$ ; 10289 reflections measured, 1514 unique reflections ( $R_{\text{int}} = 0.0291$ ); 134 refined parameters;  $R_1 = 0.0223$ ;  $wR2 = 0.0568$ . Half of the cluster is well defined in the asymmetric unit,  $\text{DMAH}^+$  cations and a few solvent water sites were refined in the disorder model. **1'**:  $\text{C}_{120}\text{H}_{267}\text{N}_{11}\text{O}_{62}\text{TeW}_{18}$ ;  $M_r = 6293.35$ ; crystal size  $0.20 \times 0.15 \times 0.04 \text{ mm}$ ;  $T = 150(2) \text{ K}$ ; triclinic; space group  $P\bar{1}$ ;  $a = 15.7634(6)$ ,  $b = 17.8793(9)$ ,  $c = 19.2987(6) \text{ \AA}$ ;  $\alpha = 106.357(4)$ ,  $\beta = 103.255(3)$ ,  $\gamma = 107.717(4)^\circ$ ;  $V = 4666.9(3) \text{ \AA}^3$ ;  $Z = 1$ ;  $\rho = 2.239 \text{ g cm}^{-3}$ ;  $\mu(\text{MoK}\alpha) = 11.265 \text{ mm}^{-1}$ ;  $F(000) = 2944$ ; 60913 reflections measured, 17289 unique reflections ( $R_{\text{int}} = 0.0436$ ); 811 refined parameters;  $R_1 = 0.035$ ;  $wR2 = 0.091$ . One cluster is well defined in the asymmetric unit,  $7\text{TBA}^+$  cations and several  $\text{CH}_3\text{CN}$  sites were refined in the disorder model. **2**:  $\text{C}_{82}\text{H}_{186}\text{N}_6\text{O}_{60}\text{Te}_1\text{W}_{18}$ ;  $M_r = 5653.27$ ; crystal size  $0.13 \times 0.09 \times 0.09 \text{ mm}$ ;  $T = 150(2) \text{ K}$ ; tetragonal; space group  $I_4$ ;  $a = 41.9907(4)$ ,  $c = 15.8445(3) \text{ \AA}$ ;  $V = 27937.3(6) \text{ \AA}^3$ ;  $Z = 8$ ;  $\rho = 2.688 \text{ g cm}^{-3}$ ;  $\mu(\text{MoK}\alpha) = 15.036 \text{ mm}^{-1}$ ;  $F(000) = 20672$ ; 97746 reflections measured; 27014 unique reflections ( $R_{\text{int}} = 0.804$ ); 1224 refined parameters;  $R_1 = 0.0413$ ;  $wR2 = 0.664$ . One cluster is well defined in the asymmetric unit,  $5\text{TBA}^+$  cations and several  $\text{CH}_3\text{CN}$  sites were refined in the disorder model. Crystal data were measured on an Oxford Diffraction Gemini CCD diffractometer using  $\text{MoK}\alpha$  radiation ( $\lambda = 0.71073 \text{ \AA}$ ). **3**:  $\text{Na}_8\text{C}_{36}\text{H}_{224}\text{N}_{18}\text{W}_{58}\text{Te}_2\text{O}_{233}$ ;  $M_r = 15740.75$ ; crystal size  $0.16 \times 0.10 \times 0.05 \text{ mm}$ ;  $T = 150(2) \text{ K}$ ; monoclinic; space group  $C2/c$ ;  $a = 25.8374(3)$ ,  $b = 27.945(2)$ ,  $c = 37.9571(14) \text{ \AA}$ ;  $\beta = 93.680(5)$ ;  $V = 27349(3) \text{ \AA}^3$ ;  $Z = 4$ ;  $\rho = 3.823 \text{ g cm}^{-3}$ ;  $\mu(\text{MoK}\alpha) = 24.608 \text{ mm}^{-1}$ ;  $F(000) = 27656$ ; 47611 reflections measured; 18889 unique reflections ( $R_{\text{int}} = 0.0813$ ); 1289 refined parameters;  $R_1 = 0.0496$ ;  $wR2 = 0.0999$ . Half cluster is well defined in the asymmetric unit,  $\text{DMAH}^+$  cations,  $\text{Na}^+$ , and several solvent water sites were refined in the disorder model. CCDC 713593 (1), 713594 (1'), 713596 (2), and 713595 (3) contain the supplementary crystallographic data for this paper. These data

- can be obtained free of charge from The Cambridge Crystallographic Data Centre via [www.ccdc.cam.ac.uk/data\\_request/cif](http://www.ccdc.cam.ac.uk/data_request/cif).
- [16] a) H. Ichida, A. Yagasaki, *J. Chem. Soc. Chem. Commun.* **1991**, 27; b) P. Gili, P. A. Lorenzo-Luis, P. Martin-Zarza, S. Dominguez, A. Sanchez, J. M. Arrieta, E. Rodriguez-Castellon, J. Jimenez-Jimenez, C. Ruiz-Perez, M. Hernandez-Molina, X. Solans, *Transition Met. Chem.* **1999**, *24*, 141; c) P. A. Lorenzo-Luis, P. Gili, A. Sanchez, E. Rodriguez-Castellon, J. Jimenez-Jimenez, C. Ruiz-Perez, X. Solans, *Transition Met. Chem.* **1999**, *24*, 686.
- [17] S. Konaka, Y. Ozawa, A. Yagasaki, *Inorg. Chem. Commun.* **2008**, *11*, 1267.
- [18] a) U. Kortz, N. K. Al-Kassem, M. G. Savelieff, N. A. Al Kadi, M. Sadakane, *Inorg. Chem.* **2001**, *40*, 4742; b) U. Kortz, M. G. Savelieff, B. S. Bassil, B. Keita, L. Nadjjo, *Inorg. Chem.* **2002**, *41*, 783.
- [19] E. M. Limanski, D. Drewes, E. Droste, R. Bohner, B. Krebs, *J. Mol. Struct.* **2003**, *656*, 17.
- [20] D. L. Long, C. Streb, Y. F. Song, S. Mitchell, L. Cronin, *J. Am. Chem. Soc.* **2008**, *130*, 1830.
- [21] C. P. Pradeep, D. L. Long, P. Kögerler, L. Cronin, *Chem. Commun.* **2008**, 4254.
- [22] E. F. Wilson, H. Abbas, B. J. Duncombe, C. Streb, D. L. Long, L. Cronin, *J. Am. Chem. Soc.* **2008**, *130*, 13876.
- [23] T. Lehmann, J. Fuchs, *Z. Naturforsch. B* **1988**, *43*, 89.
- [24] H. N. Miras, J. Yan, D. L. Long, L. Cronin, *Angew. Chem.* **2008**, *120*, 8548; *Angew. Chem. Int. Ed.* **2008**, *47*, 8420.
- [25] B. E. Douglas, D. H. McDaniel, J. J. Alexander, *Concepts and Models of Inorganic Chemistry*, Wiley, New York, **1993**.
- [26] Controlled fragmentation can be induced by collision-induced dissociation at high energies, enabling us to establish how cluster decomposition would occur. The absence of such peaks, and the clear observation of the transformation of  $\{W_{18}Te^{VI}\}$  to  $\{W_{18}Te^{IV}\}$  is very strong evidence suggesting the cluster remains intact during the reduction process.